A Hybrid UWPW-FEM Technique for Vibroacoustic Analysis of Panels Subject to a Turbulent Boundary Layer Excitation

Mahmoud Karimi, Laurent Maxit, Paul Croaker, Olivier Robin, Alex Skvortsov, Noureddine Atalla, Nicole Kessissoglou

Abstract A hybrid uncorrelated wall plane wave (UWPW) and finite element method (FEM) technique is introduced to the predict vibroacoustic response of a panel under turbulent boundary layer (TBL) excitation. The spectrum of the wall pressure fluctuations is evaluated from the TBL parameters and by using semi-empirical models from literature. TBL parameters can be estimated by different means, using theoretical formula, Reynolds-averaged Navier Stokes (RANS) simulations or experimental data. The wall pressure field (WPF) underneath the TBL is then synthesized by realisations of uncorrelated wall plane waves. The FEM is employed to compute the structural and acoustic responses of the panel for each realisation of uncorrelated wall plane waves. The responses are then obtained from an ensemble average of the different realisations. Selection criteria for cut-off wavenumber, mesh size and number of realisation are discussed. Two simply-supported baffled panels under TBL excitation are examined. Numerical results are compared with analytical results using the sensitivity functions of the panels, showing excellent agreement.

Mahmoud Karimi
Centre for Audio, Acoustics and Vibration, University of Technology Sydney, Sydney, Australia. e-mail: Mahmoud.Karimi@uts.edu.au

Laurent Maxit
Univ Lyon, INSA-Lyon, Laboratoire Vibrations-Acoustique (LVA), 25 bis, av. Jean Capelle, F-69621, Villeurbanne Cedex, France e-mail: Laurent.Maxit@insa-lyon.fr

Paul Croaker and Nicole Kessissoglou
School of Mechanical and Manufacturing Engineering, The University of New South Wales, Sydney, Australia e-mail: P.Croaker@unsw.edu.au, N.Kessissoglou@unsw.edu.au

Olivier Robin and Noureddine Atalla
Groupe d'Acoustique de l'Université de Sherbrooke, Université de Sherbrooke, Sherbrooke, J1K 2R1, Canada e-mail: Olivier.Robin@USherbrooke.ca, Noureddine.Atalla@USherbrooke.ca

Alex Skvortsov and Paul Croaker
Maritime Division, Defence Science and Technology, Melbourne, Australia e-mail: Alex.Skvortsov@dst.defence.gov.au, Paul.Croaker@dst.defence.gov.au

1 Introduction

Predicting the vibroacoustic responses of structures subject to random pressure fields is important in naval and aerospace industries. The correct prediction of the vibrational response is crucial to minimise structural fatigue as well as structure-borne radiating noise [1–3]. A large and growing body of literature has investigated the vibrational responses of plates excited by a turbulent flow field in air, including analytical models of infinite and finite plates [4, 5], numerical models [5–11], and from experiments [10]. Further, many researchers have investigated the vibroacoustic responses of planar structures excited by turbulent flow, for example, see Refs. [2–8, 12–26]. To predict the vibroacoustic response of a structure excited by a TBL, the turbulent pressure field should be obtained on the surface of the structure. This can be done using direct numerical simulation (DNS) or large eddy simulation (LES). However, these simulations are computationally very expensive. An alternative approach involves a steady-state RANS solution to predict the TBL parameters [27,28]. Researchers have shown an increased interest in using RANS. This is due to its capabilities to predict TBL parameter mean values with good fidelity. These parameters can then be used as an input to analytical or semi-empirical models to predict the WPF under the TBL [29–31].

The vibroacoustic response of a structure excited by a TBL depends on the cross spectrum density (CSD) function of the wall pressure fluctuations. Therefore, to correctly describe the partial correlation of the excitation, a large number of frequency response functions needs to be obtained for the distributed points on the surface of structure [7,9]. To describe the random WPF, a statistical model is required. The coupling between the statistical model and a deterministic numerical model of the structure represents a difficulty in the calculation process. In this work, a hybrid approach is proposed to overcome this difficulty by coupling the UWPW technique to simulate the WPF underneath a TBL and a deterministic method to model the structural-acoustic domain. A deterministic input load to the vibroacoustic solver based on the FEM is computed from each realisation of the WPF. The vibroacoustic response of the panel is then obtained from an ensemble average of the different panel responses. The major advantage of the UWPW technique is that it is a non-intrusive technique which produces deterministic loads. As such, any element-based numerical method can be used in conjunction with the UWPW technique to examine vibroacoustic response of the structure under TBL excitation. For example, the FEM as well as the boundary element method (BEM) can be employed to analyse structural and acoustic responses of the structure subject to a TBL excitation [11, 32, 33].

In this work, criteria for selecting calculation parameters in the hybrid UWPW-FEM technique such as cut-off wavenumber, mesh size and number of realisations are initially discussed. To demonstrate the hybrid technique, two case studies are considered corresponding to two different simply supported plates made of aluminium. The first case study only examines the vibrational response. Acoustic radiation from a panel is also studied in the second case study. Numerical results are compared with analytical results using sensitivity functions, showing excellent agreement. The analytical method is limited in its application to simple panels with simply supported

boundary conditions. In contrast, the numerical method can be applied to complex structures with arbitrary boundary conditions.

2 Numerical formulation

Figure 1 shows an elastic rectangular finite baffled panel excited by a turbulent flow field. It is assumed that the TBL is homogeneous, stationary and fully developed over the panel surface.

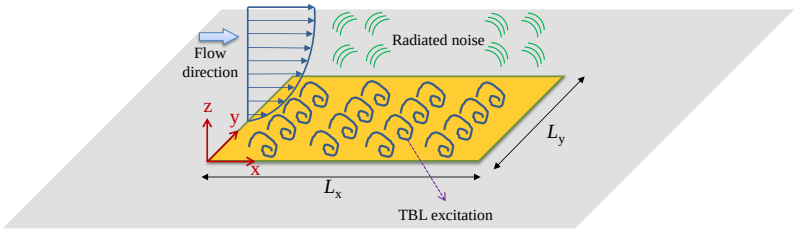

Fig. 1 An elastic baffled panel under TBL excitation

The UWPW technique recently introduced by Maxit [32] is used herein to simulate the pressure field beneath a TBL. The pressure beneath a TBL for the l^{th} realisation can be represented by a set of UWPWs at the q^{th} node, $\mathbf{x}^q = (x^q, y^q)$, of an FEM mesh as follows [11, 32, 34]

$$p^l_{\text{inc}}(\mathbf{x}^q, \omega) = \sum_{i=1}^{N_x} \sum_{j=1}^{N_y} \sqrt{\frac{\phi_{pp}(k_x^i, k_y^j, \omega)\delta k_x \delta k_y}{4\pi^2}}\, e^{\mathrm{i}(k_x^i x^q + k_y^j y^q + \varphi_{ij}^l)}, \tag{1}$$

where ω is the angular frequency and φ is a random phase uniformly distributed in $[0 \;\; 2\pi]$. Criteria for selecting the wavenumber resolutions δk_x, δk_y as well as the truncated numbers of plane waves N_x and N_y are discussed in section 3. The CSD can be expressed in terms of the ASD of the pressure field $S_{pp}(\omega)$ and the normalized CSD of the pressure field $\tilde{\phi}_{pp}(\mathbf{k}, \omega)$ as follows [32, 35]

$$\phi_{pp}(\mathbf{k}, \omega) = \Psi_{pp}(\omega) \left(\frac{U_c}{\omega}\right)^2 \tilde{\phi}_{pp}(\mathbf{k}, \omega), \tag{2}$$

where U_c is the convective velocity. Using equation (1) as the deterministic load, the FEM is now implemented to simultaneously compute the l^{th} realisation of the structural displacement $\mathbf{u}^l$ and the radiated pressure $\mathbf{p}^l$ by solving the following fully coupled structural-acoustic equations [36]

$$\underbrace{\begin{bmatrix} -\omega^2\mathbf{M}_s + \mathbf{K}_s & -\mathbf{H}_{fs} \\ -\omega^2\rho_f c_f^2 \mathbf{H}_{fs}^{\mathrm{T}} & -\omega^2\mathbf{M}_f + \mathbf{K}_f \end{bmatrix}}_{\mathbf{A}} \begin{bmatrix} \mathbf{u}^l \\ \mathbf{p}^l \end{bmatrix} = \begin{bmatrix} \mathbf{f}_s^l \\ \mathbf{f}_f \end{bmatrix}, \tag{3}$$

where $\mathbf{K}$, $\mathbf{H}$ and $\mathbf{M}$ are respectively stiffness, coupling and mass matrices. Subscripts s and f respectively refer to the structure and fluid. $\mathbf{f}_s^l$ is the structural force vector corresponding to the l^{th} realisation of the TBL pressure field given by equation (1). $\mathbf{f}_f$ is the load from acoustic sources in the fluid domain, which is zero for the current case. After the inverse of the coefficient matrix $\mathbf{A}$ is obtained, the panel displacement response and radiated pressure can be computed for each realisation as follows

$$\begin{bmatrix} \mathbf{u}^l \\ \mathbf{p}^l \end{bmatrix} = \mathbf{A}^{-1} \begin{bmatrix} \mathbf{f}_s^l \\ \mathbf{0} \end{bmatrix}. \tag{4}$$

The ASD of the panel velocity S_{vv}, the cross spectrum between the sound pressure and the fluid particle velocity S_{pv_f} due to the TBL excitation are then calculated from the ensemble average of the different realisations by

$$S_{vv} = -\omega^2 \mathrm{E}\left[\mathbf{u}^l \mathbf{u}^{*l}\right]_l, \tag{5}$$

$$S_{pv_f} = \mathrm{E}\left[\mathbf{p}^l \mathbf{v}_{\mathbf{f}}^{*l}\right]_l, \tag{6}$$

where $\mathrm{E}[\ ]$ represents the ensemble average of the realisations. The cross spectrum between the sound pressure and the fluid particle velocity can be used to determine the radiated sound power [33].

The computational steps for the proposed hybrid technique is illustrated in Figure 2. First, an FEM mesh is created from the geometry of the structure. To estimate the TBL parameters over the surface of the structure for a given geometry and flow condition, a RANS simulation, theoretical formula or experimental data can be employed. The TBL parameters are then substituted into semi-empirical models to evaluate the CSD of the WPF. The deterministic WPF is synthesized using the UWPW technique. The WPF is then used as an input to the FEM solver to calculate the structural and acoustic responses. This process is repeated for each realisation of the WPF. Finally, the vibroacoustic response of the system is obtained from an ensemble average of the different realisations of the WPFs at each frequency.

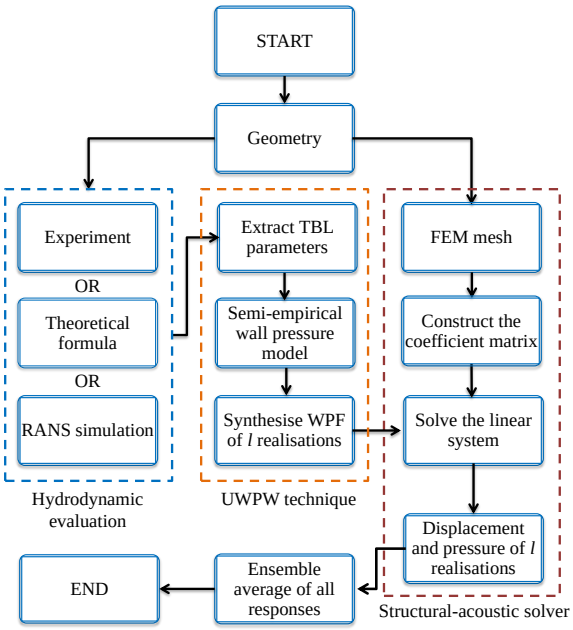

Fig. 2 Flowchart outlining the computational process of the hybrid UWPW-FEM technique

3 Selection of calculation parameters

3.1 Determination of cut-off wavenumbers and wavenumber resolutions

To obtain the panel response, one needs to truncate the wavenumber domain in the x and y directions for equation (1). It was shown that in the vibrational response, for the frequencies of interest well above the aerodynamic coincidence frequency, the wavenumbers below or close to the flexural wavenumber of the plate are dominant [7, 25, 32]. At the aerodynamic coincidence frequency, the flexural wavenumber $k_p = (\omega\sqrt{\rho_s h/D})^{1/2}$ equals the convective wavenumber $k_c = \omega/U_c$ and the TBL strongly excites the structure. The aerodynamic coincidence frequency is given by $f_c = U_c^2\sqrt{\rho_s h/D}/(2\pi)$ [25]. Hence, a cut-off wavenumber of $2k_{p,\max}$ was used in both the streamwise and spanwise directions, where $k_{p,\max} = (\omega_{\max}\sqrt{\rho_s h/D})^{1/2}$ is the flexural wavenumber of the plate at the maximum frequency of interest, denoted by $\omega_{\max}$. This criterion was chosen based on the fact that for frequencies well above the aerodynamic frequency, the structural response of a panel excited by a TBL can be obtained by neglecting the effect of the convected ridge as confirmed in Refs [11,32]. The criterion defined here takes into account the effect of the convective ridge at lower frequencies as the cut-off wavenumber was defined as twice the flexural wavenumber at the highest frequency of interest. The validity of this criterion for evaluating the

acoustic response of a panel excited by a TBL was recently examined by Karimi et al. [33]. It was shown that this criterion can be employed to predict the vibroacoustic response of a panel under a TBL excitation.

To represent the spatial variations in the wavenumber space of the wall pressure spectrum, a constant wavenumber resolution can be determined through a trial and error process [11, 32]. Alternatively, a frequency dependent increment in the wavenumber domain could be chosen similar to the work by Karimi et al. [34] for acoustic scattering prediction.

3.2 Criterion for the mesh size

The mesh size must be defined such that it enables us to properly describe the hydrodynamic field on the surface of structure. This requires taking into account the spatial distribution of the CSD function of the surface pressure. To synthesize the WPF, the Nyquist sampling theorem for space and wavenumber was adopted. The sampling wavenumber is given by [9]

$$k_s = \frac{2\pi}{\Delta h}, \tag{7}$$

where Δh is the element size. According to the Nyquist theorem, the sampling wavenumber must be at least twice the highest wavenumber of interest, that is, $k_s = 2k_{p,\max}$. Substituting this expression into equation (7), the mesh size is given by

$$\Delta h = \frac{\pi}{k_{p,\max}}. \tag{8}$$

Further, to properly resolve structural modes by considering the FEM mesh size requirement of at least 10 elements per wavelength, the grid size in the streamwise and spanwise directions can be defined as follows

$$\Delta x = \Delta y = \min\left\{\frac{\lambda_{p,\max}}{10}, \frac{\pi}{k_{p,\max}}\right\}, \tag{9}$$

where Δx, Δy are the element size in the x and y directions and $\lambda_{p,\max}$ is the flexural wavenumber of the plate at the maximum frequency of interest. Since $k_{p,\max} = 2\pi/\lambda_{p,\max}$, the mesh size criterion is given by $\Delta x = \Delta y = \lambda_{p,\max}/10$.

4 Verification of the UWPW-FEM technique

To demonstrate the UWPW-FEM technique, two case studies comprising rectangular baffled panels with simply supported boundary conditions excited by a TBL are examined [11]. Dimensions and material properties of both panels are given in

Table 1. The first case study investigates the vibrational response of panel A. The second case study examines the acoustic response of panel B. Numerical results obtained using the UWPW-FEM technique for the both panels are compared with analytical results. An analytical model based on sensitivity functions of the panel was used as a reference solution to verify the numerical method [11, 33]. The fluid density and the kinematic viscosity were set to 1.225 kg/m^3 and 1.5111×10^{-5} m^2/s, respectively. The simulations were conducted using Matlab on a desktop personal computer with 32 GB of RAM and a total of four physical cores. For the UWPW-FEM technique, the WPF was synthesized in Matlab and then imported as a load to the FEM model of the panel in the commercial software COMSOL Multiphysics (v5.3a) using Matlab LiveLink.

Table 1. Dimensions and material properties of the panels

Parameter	Panel A	Panel B
Young's modulus E (GPa)	70	68.9
Poisson's ratio ν	0.3	0.3
Density ρ_s (kg/m^3)	2700	2740
Length L_x (mm)	480	600
Width L_y (mm)	420	525
Thickness h (mm)	3.17	2.4
Damping loss factor η	0.005	0.01

4.1 Synthetic pressure field

To obtain the WPF, the Goody model was used to evaluate the ASD function of the WPF [11, 37]. Note that $\Psi_{pp}(\omega)$ is a one-sided angular frequency spectrum. Hence $\Psi_{pp}(\omega)$ was multiplied by 2π to convert it to a one-sided cyclic frequency spectrum density $\Psi_{pp}(f)$. For the normalized CSD function, the Mellen model was employed [38]. The TBL parameters were calculated based on theoretical formula for a flat plate from literature and are given in Table 2 [11]. The convective velocity U_c was approximated as follows [11, 39]

$$U_c \cong U_\infty(0.59 + 0.3e^{-0.89\delta^*\omega/U_\infty}), \tag{10}$$

where U_∞ is the free flow velocity and δ^* is boundary layer displacement thickness. Employing the Goody and Mellen models, different realisations of the WPF were synthesized on the surface of panel A using equation (1). Figure 3 shows the visualization of two realisations of the surface pressure field at two discrete resonance frequencies corresponding to 177 Hz and 1005 Hz, for a flow speed of 40 m/s. Figure 3(a) shows that at low frequencies, a coarse mesh can resolve the waves as they have larger wavelengths. However, at higher frequencies, a finer mesh is needed to properly describe and synthesize the WPF for plane waves with short wavelengths (Figure 3(b)). In this work, the criteria defined in section 3.2 for the mesh size en-

sures that the plane waves with the shortest wavelength corresponding to the highest frequency of interest are adequately resolved.

Table 2. TBL parameters for Panel A at flow speeds of 40 m/s, 60 m/s and 80 m/s

Parameter	U_∞ = 40 m/s	U_∞ = 60 m/s	U_∞ = 80 m/s
TBL thickness δ (m)	0.0349	0.0322	0.0304
TBL displacement thickness δ^* (m)	0.0044	0.0041	0.0038
Wall shear stress τ (Pa)	2.5228	5.2341	8.7848

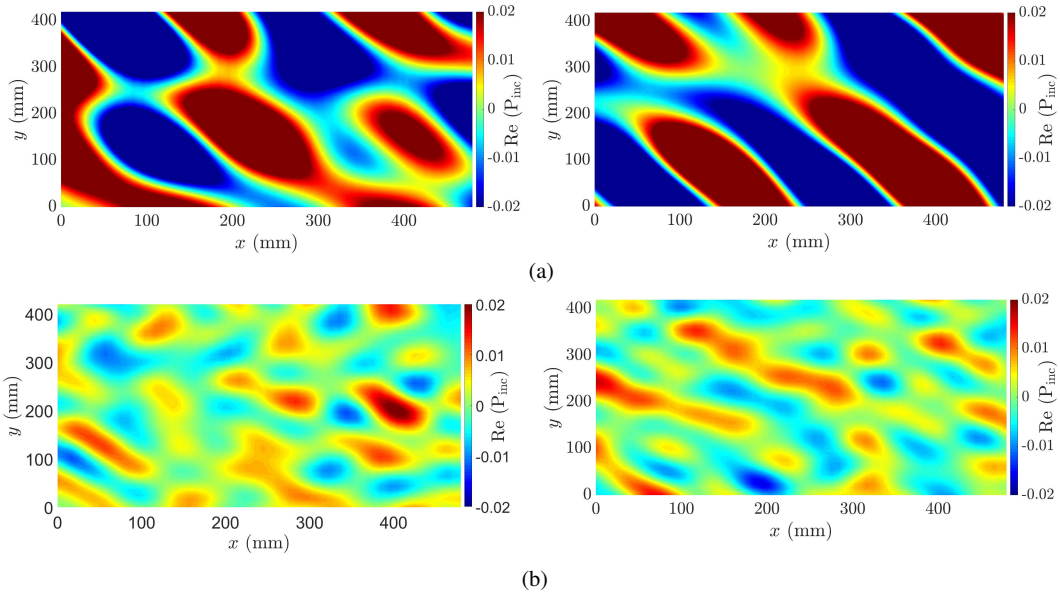

(a)

(b)

Fig. 3 Two realisations of the WPF (in Pascal) using the Mellen and Goody models for a flow speed of 40 m/s at (a) 177 Hz and (b) 1005 Hz

4.2 Effect of the number of realisations

The number of realisations used in the calculation process has significant effect on the accuracy of the UWPW method. This effect has been investigated for acoustic scattering prediction [34], vibrational analysis of a panel [11] and acoustic radiation from a baffled panel [33]. In all of these cases, it was confirmed that 30 realisations is sufficient to obtain the response of the system with the maximum estimated error less than 1 dB for the frequency range considered. For example, the effect of the number of realisations on the structural response of panel A excited by a TBL at a flow speed of 40 m/s is shown in Figure 4. The spectral level predicted using 30 different realisations is shown in grey lines and the black line represents the predicted results by averaging of 30 realisations. Figure 5 compares the velocity

spectra obtained numerically using the average of 30 realisations with analytical results. The analytical solution described in Ref [11] is provided as a reference solution. It can be observed from Figures 4 and 5 that the numerical results become smoother and converge quickly towards the reference solution by increasing the number of realisations.

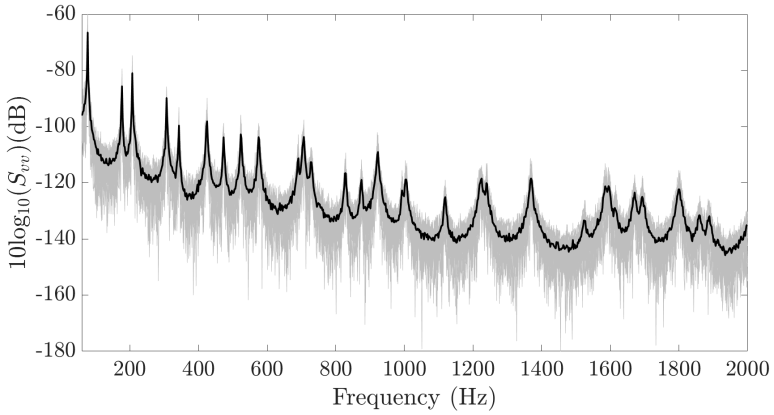

Fig. 4 ASD of the panel velocity predicted numerically using the UWPW-FEM technique for 30 realisations (grey lines), as well as predicted using the average of 30 realisations (black line), for a flow speed of 40 m/s (dB ref. 1 $(\text{m/s})^2/\text{Hz}$)

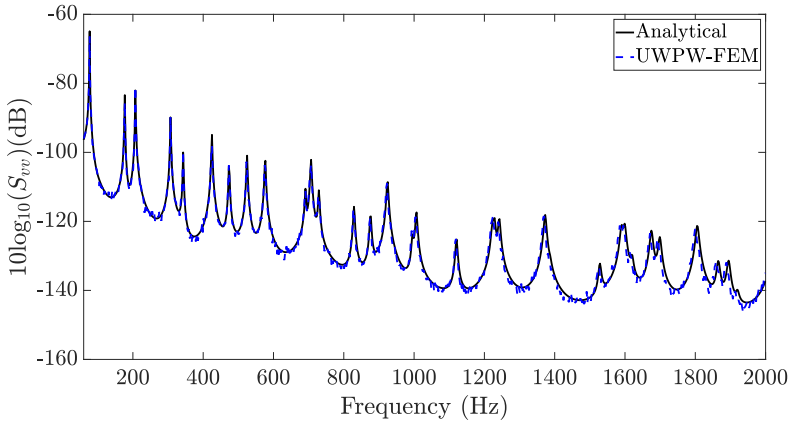

Fig. 5 ASD of the panel velocity predicted numerically using the UWPW-FEM technique by averaging of 30 realisations, as well as predicted analytically, for a flow speed of 40 m/s (dB ref. 1 $(\text{m/s})^2/\text{Hz}$)

4.3 Structural response

To predict the panel responses, the synthesized WPF was applied as a load to the structural-acoustic solver. Figure 6 presents the predicted velocity spectra using the UWPW-FEM technique as well as the analytically calculated velocity spectra for panel A at flow speeds of 60 m/s and 80 m/s. The vibration of the panel was obtained at ($x = 0.3$ m, $y = 0.33$ m, $z = 0$ m) on the panel surface with respect to the coordinate system shown in Figure 1. The numerical results are in excellent agreement with analytical results. As expected, with increasing flow speed, the magnitude of the vibrational response of the panel increases. For the parameters chosen here, the aerodynamic coincidence frequency is 66 Hz and 117 Hz for flow speeds of 60 m/s and 80 m/s, respectively.

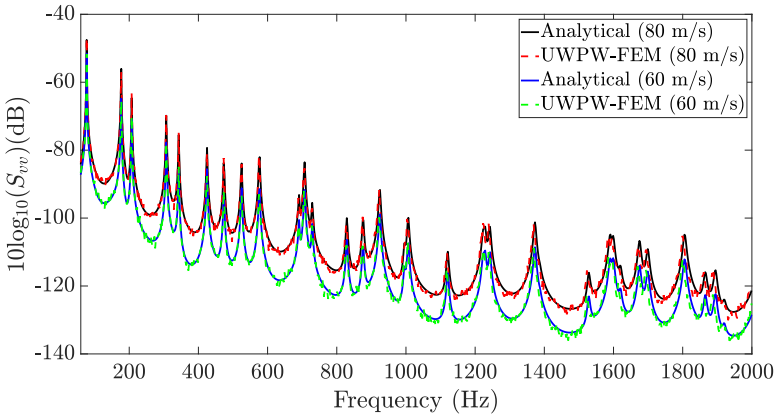

Fig. 6 ASD of the panel velocity for a simply supported plate predicted using the UWPW-FEM technique and analytical formulation, for flow speeds of 60 m/s and 80 m/s (dB ref. 1 $(\text{m/s})^2/\text{Hz}$)

4.4 Acoustic response

The hybrid technique was applied to predict the acoustic response of panel B with simply-supported boundary conditions and excited by a TBL. The panel was tested in an anechoic wind tunnel at the Université de Sherbrooke [40]. The experiments were conducted at a free flow speed of 40 m/s. The wall pressure fluctuations of the turbulent flow generated over the baffle were measured by a flush-mounted microphone array as described in [25, 40]. The Mellen model was fitted to the measured WPF using the least square method to estimate the decay rates, α_x and α_y, and the convective velocity U_c. The experimentally fitted Mellen model as well as the measured autospectrum of the WPF, presented in Ref [33], were used for evaluation of the CSD function of the WPF. Numerical prediction of the acoustic power is

compared with the analytical results in Figure 7. It can be seen that numerical results are in excellent agreement with analytical results. Readers are referred to Refs [11, 33] for detailed discussions on validation of the numerical results with experimental data.

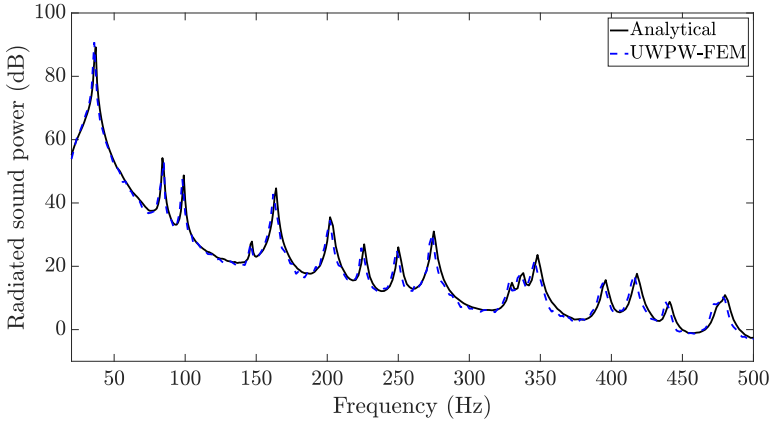

Fig. 7 Sound power spectrum level predicted using the UWPW-FEM technique and analytical formulation for flow speed of $U_\infty = 40$ m/s (dB ref. 1×10^{-12} W/Hz).

5 Conclusions

An uncorrelated wall plane wave technique has been presented to deterministically synthesize the WPF underneath a TBL from the CSD of the WPF expressed in the frequency-wavenumber domain. The pressure field was then used as an input to an FEM solver to predict vibroacoustic responses of panels under TBL excitation. One of the main advantages of using the non-intrusive UWPW technique in the vibroacoustic solver is that the deterministic WPF is calculated at each FEM nodal point, and can be applied as an input to the FEM or other element-based approaches to evaluate the panel structural-acoustic response. Further, it was shown that the hybrid UWPW-FEM technique produced converged results using small number of realisations. An analytical method based on the sensitivity function was employed to verify the numerically obtained vibroacoustic results for two different simply-supported panels. It was shown that the hybrid UWPW-FEM technique can be confidently used to predict the vibroacoustic responses of panels excited by turbulent flow. Whilst the case studies presented here comprise simple panels with simply supported conditions, the proposed method can be applied to study the vibroacoustic responses of complex panels with arbitrary boundary conditions under TBL excitation. For example, the vibroacoustic response of a stiffened plate under TBL excitation has

been recently analysed in Ref [33] using the hybrid UWPW-FEM technique. The technique is also well adapted for investigating the effects of design modifications. Once the WPF fields of the different realisations have been calculated, they can be applied to different panel models to study the influence of the design on the vibroacoustic response. Moreover, in the presence of complex flow conditions, a RANS simulation can be performed for more accurate calculation of the TBL parameters.

Acknowledgements This research was supported by the Australian Government through the Australian Research Council's Discovery Early Career Project funding scheme (project DE190101412).

References

1. R.C. Leibowitz. Vibroacoustic response of turbulence excited thin rectangular finite plates in heavy and light fluid media. *J Sound Vib*, 40(4):441 – 495, 1975.
2. E. Ciappi, S. De Rosa, F. Franco, J.L. Guyader, and S.A. Hambric. *Flinovia - Flow Induced Noise and Vibration Issues and Aspects: A Focus on Measurement, Modeling, Simulation and Reproduction of the Flow Excitation and Flow Induced Response*. EBL-Schweitzer. Springer International Publishing Switzerland, 2014.
3. E. Ciappi, S. De Rosa, F. Franco, J.L. Guyader, S.A. Hambric, R.C.K. Leung, and A.D. Hanford. *Flinovia-Flow Induced Noise and Vibration Issues and Aspects-II: A Focus on Measurement, Modeling, Simulation and Reproduction of the Flow Excitation and Flow Induced Response*. Springer International Publishing Switzerland, 2018.
4. W. Strawderman. Turbulence-induced plate vibrations: an evaluation of finite and infinite plate models. *J Acoust Soc Am*, 46(5B):1294–1307, 1969.
5. S. De Rosa and F. Franco. Exact and numerical responses of a plate under a turbulent boundary layer excitation. *J Fluids Struct*, 24(2):212–230, 2008.
6. F. Birgersson, N. S. Ferguson, and S. Finnveden. Application of the spectral finite element method to turbulent boundary layer induced vibration of plates. *J Sound Vib*, 259(4):873–891, 2003.
7. S. Hambric, Y. Hwang, and W. Bonness. Vibrations of plates with clamped and free edges excited by low-speed turbulent boundary layer flow. *J Fluids Struct*, 19(1):93–110, 2004.
8. F. Birgersson and S. Finnveden. A spectral super element for modelling of plate vibration. Part 2: turbulence excitation. *J Sound Vib*, 287(1-2):315–328, 2005.
9. C. Hong and K. Shin. Modeling of wall pressure fluctuations for finite element structural analysis. *J Sound Vib*, 329(10):1673–1685, 2010.
10. E. Ciappi, S. De Rosa, F. Franco, P. Vitiello, and M. Miozzi. On the dynamic behavior of composite panels under turbulent boundary layer excitations. *J Sound Vib*, 364:77–109, 2016.
11. M Karimi, P Croaker, L Maxit, O Robin, A Skvortsov, S Marburg, and N Kessissoglou. A hybrid numerical approach to predict the vibrational responses of panels excited by a turbulent boundary layer. *J Fluids Struct*, 92:102814, 2020.
12. W. Strawderman and R. Christman. Turbulence-induced plate vibrations: Some effects of fluid loading on finite and infinite plates. *J Acoust Soc Am*, 52(5B):1537–1552, 1972.
13. H. G. Davies. Sound from turbulent-boundary-layer-excited panels. *J Acoust Soc Am*, 49(3B):878–889, 1971.
14. G. Cousin. Sound from TBL-induced vibrations. In *4th AIAA/CEAS Aeroacoustics Conference*, page 2216, Toulouse, France, June 1998.
15. F. Han, L. Mongeau, and R. Bernhard. A model for the vibro-acoustic response of plates excited by complex flows. *J Sound Vib*, 246(5):901–926, 2001.
16. C. Maury, P. Gardonio, and S. Elliott. A wavenumber approach to modelling the response of a randomly excited panel, Part I: General theory. *J Sound Vib*, 252(1):83–113, 2002.

17. C. Maury, P. Gardonio, and S. Elliott. A wavenumber approach to modelling the response of a randomly excited panel, Part II: Application to aircraft panels excited by a turbulent boundary layer. *J Sound Vib*, 252(1):115–139, 2002.
18. D. Mazzoni. An efficient approximation for the vibro-acoustic response of a turbulent boundary layer excited panel. *J Sound Vib*, 264(4):951–971, 2003.
19. J. Park, L. Mongeau, and T. Siegmund. An investigation of the flow-induced sound and vibration of viscoelastically supported rectangular plates: experiments and model verification. *J Sound Vib*, 275(1-2):249–265, 2004.
20. E. Ciappi, F. Magionesi, S. De Rosa, and F. Franco. Hydrodynamic and hydroelastic analyses of a plate excited by the turbulent boundary layer. *J Fluids Struct*, 25(2):321–342, 2009.
21. B. Liu. Noise radiation of aircraft panels subjected to boundary layer pressure fluctuations. *J Sound Vib*, 314(3-5):693–711, 2008.
22. B. Liu, L. Feng, A. Nilsson, and M. Aversano. Predicted and measured plate velocities induced by turbulent boundary layers. *J Sound Vib*, 331(24):5309–5325, 2012.
23. J. Rocha. Sound radiation and vibration of composite panels excited by turbulent flow: analytical prediction and analysis. *Shock and Vibration*, 2014, 2014.
24. C. Marchetto, L. Maxit, O. Robin, and A. Berry. Vibroacoustic response of panels under diffuse acoustic field excitation from sensitivity functions and reciprocity principles. *J Acoust Soc Am*, 141(6):4508–4521, 2017.
25. C. Marchetto, L. Maxit, O. Robin, and A. Berry. Experimental prediction of the vibration response of panels under a turbulent boundary layer excitation from sensitivity functions. *J Acoust Soc Am*, 143(5):2954–2964, 2018.
26. X. Zhao, B. AI, Z Liu, and D. Li. A scaling procedure for panel vibro-acoustic response induced by turbulent boundary layer. *J Sound Vib*, 380:165–179, 2016.
27. C. Bailly, P. Lafon, and S. Candel. Subsonic and supersonic jet noise predictions from statistical source models. *AIAA J*, 35(11):1688–1696, 1997.
28. L. Peltier and S. Hambric. Estimating turbulent-boundary-layer wall-pressure spectra from CFD RANS solutions. *J Fluid Struct*, 23(6):920–937, 2007.
29. W.K. Blake. *Mechanics of flow-induced sound and vibration: Complex flow-structure interactions*. Applied Mathematics and Mechanics Series. Academic Press, 1986.
30. Y. T. Lee, W. K. Blake, and T. M. Farabee. Modeling of wall pressure fluctuations based on time mean flow field. *J Fluid Eng*, 127(2):233–240, 2005.
31. L. Chen and I. R. MacGillivray. Prediction of trailing edge noise based on Reynolds Averaged Navier Stokes solution. *AIAA J*, 52(12):2673–2682, 2014.
32. L. Maxit. Simulation of the pressure field beneath a turbulent boundary layer using realizations of uncorrelated wall plane waves. *J Acoust Soc Am*, 140(2):1268–1285, 2016.
33. M. Karimi, L. Maxit, P. Croaker, O. Robin, A. Skvortsov, S. Marburg, N. Atalla, and N. Kessissoglou. Analytical and numerical prediction of acoustic radiation from a panel under turbulent boundary layer excitation. *J Sound Vib*, 2020, 10.1016/j.jsv.2020.115372.
34. M. Karimi, P. Croaker, A. Skvortsov, D. Moreau, and N. Kessissoglou. Numerical prediction of turbulent boundary layer noise from a sharp-edged flat plate. *Int J Numer Meth Fl*, 90:522–543, 2019.
35. W. R. Graham. A comparison of models for the wavenumber–frequency spectrum of turbulent boundary layer pressures. *J Sound Vib*, 206(4):541–565, 1997.
36. P. Davidsson. *Structure-acoustic analysis; finite element modelling and reduction methods*. PhD thesis, Division of Structural Mechanics, LTH, Lund University, Lund, Sweden, 2004.
37. M. Goody. Empirical spectral model of surface pressure fluctuations. *AIAA J*, 42:1788–1793, 2004.
38. R. Mellen. Wave-vector filter analysis of turbulent flow. *J Acoust Soc Am*, 95(3):1671–1673, 1994.
39. MK Bull. Wall-pressure fluctuations associated with subsonic turbulent boundary layer flow. *J Fluid Mech*, 28(4):719–754, 1967.
40. M. Jenzri, O. Robin, and N. Atalla. Vibration of and radiated acoustic power from a simply-supported panel excited by a turbulent boundary layer excitation at low Mach number. *Noise Control Eng J*, 67(4):241–251, 2019.